TÜBİTAK

Turkish Journal of Medical Sciences

http://journals.tubitak.gov.tr/medical/

Research Article

Turk J Med Sci
(2013) 43: 84-92
© TÜBİTAK
doi:10.3906/sag-1202-18

The MR imaging features and the analyses of quantitative parameters in cases with surgically repaired tetralogy of Fallot

Salih HAMCAN[1], Bülent KARAMAN[1], Bilal BATTAL[1,*], Veysel AKGÜN[2], Kemal KARA[1], Tuncay HAZIROLAN[3], Uğur BOZLAR[1]

[1]Department of Radiology, Gülhane Military Medical School, Ankara, Turkey
[2]Department of Radiology, Gölcük Military Hospital, Kocaeli, Turkey
[3]Department of Radiology, Faculty of Medicine, Hacettepe University, Ankara, Turkey

Received: 07.02.2012 • **Accepted:** 20.06.2012 • **Published Online:** 18.01.2013 • **Printed:** 18.02.2013

Aim: To present postoperative cardiac magnetic resonance (CMR) imaging features of cases of surgically repaired tetralogy of Fallot (TOF) and to evaluate the relationship among data used in follow-up procedures, such as right ventricular ejection fraction (RV-EF), pulmonary regurgitation fraction (PRF), and the degree of right ventricular (RV) dysfunction.

Materials and methods: Fourteen patients (9 males and 5 females; mean age 11.9 ± 3.6 years) with surgically repaired TOF who were admitted to our clinic for follow-up CMR imaging between July 2008 and September 2011 were included in the study. A protocol that consisted of cine steady-state free precession (SSFP) and velocity-encoding phase-contrast and contrast-enhanced MR angiography techniques was performed for every patient with 1.5-T equipment. PRF, RV function, and vascular pathologies were evaluated with phase-contrast velocity-encoding MR technique, cine SSFP sequence, and contrast-enhanced MR angiography, respectively. The relationship among RV-EF, PRF, and the degree of RV dysfunction were evaluated by using chi-square and Mann–Whitney U tests.

Results: Various findings such as pulmonary regurgitation, decreased RV-EF, RV enlargement, increased trabeculation of RV wall, deterioration of the RV function, RV outflow tract dilatation, dyskinesia of the interventricular septum, and tricuspid regurgitation were observed. Mean PRF was 41.4 ± 5.4% (range: 29% to 48%), while mean RV-EF was 42.3 ± 9.2% (range: 29.3% to 58.5%). There was no statistically significant relationship between the degree of PRF and the degree of RV dysfunction (P = 0.147, chi-square test, Spearman's rho= –0.158).

Conclusion: CMR imaging is an adequate method in follow-up of quantitative measurements of parameters such as PRF and RV dysfunction in addition to morphological features, and in determination of the possible complications in patients with surgically repaired TOF. In these patients, the degree of PRF does not correlate with the degree of RV dysfunction.

Key words: Cardiac, magnetic resonance, tetralogy of Fallot, pulmonary regurgitation, ejection fraction

1. Introduction

Tetralogy of Fallot (TOF) is one of the cyanotic heart diseases and accounts for 6%–10% of all congenital heart diseases (1,2). Ventricular septal defect (VSD), overriding aorta, stenosis of the right ventricular outflow tract (RVOT), and right ventricular (RV) hypertrophy are the components of this condition. Blalock and Taussing defined and performed the first palliative surgical treatment in TOF patients by forming a shunt between the pulmonary artery and systemic arteries in 1945 (3). Lillehei et al. accomplished full surgical repair for the first time in 1954 (4). The surgical repair of this condition has good prognostic value and decreases early mortality risk to a value lower than 2% (5). The mortality risk of the operation was formerly about 50%, but recently it has decreased to 2%. Due to advances in surgical repair technique, the number of the patients with surgically repaired TOF has increased. Complications such as RV dilatation, pulmonary regurgitation (PR), residual atrial septal defect and VSD, tricuspid regurgitation (TR), aneurysm of the RVOT, pulmonary artery stenosis, atrial/ventricular arrhythmias, congestive heart failure, and sudden death can be encountered during long-term postoperative follow-up of these patients. Most of the complications are well tolerated during childhood and adolescence. However, arrhythmia, congestive heart failure, exercise intolerance, and sudden death can be seen, especially in the third decade after surgery (6).

* Correspondence: bilbat_23@yahoo.com

Chronic severe pulmonary regurgitation may cause RV dilatation and pulmonary insufficiency. Pulmonary insufficiency is one of the complications that can be treated in patients with surgically repaired TOF. Although there are many studies focused on this topic, further ones are still needed to reveal the appropriate indication, method, and optimal timing for pulmonary valve replacement.

Besides morphologic assessment, ventricular function and volume measurements can be performed by cardiac magnetic resonance (CMR) imaging. Pulmonary regurgitation fraction (PRF) measurement can also be performed by using phase-contrast velocity-encoding magnetic resonance (MR) techniques, and vascular pathologies can be assessed by an MR angiography. CMR is a noninvasive technique that does not require ionizing radiation or nephrotoxic iodinated contrast media (7,8). By using this operator-independent technique, the right ventricle and pulmonary valves can be effectively evaluated, and both qualitative and quantitative assessments can be performed. Familiarity with the anatomic features of the TOF, surgical techniques, postoperative changes, and complications has an important role in performing an adequate interpretation of the CMR.

In this study, we aimed to present postoperative CMR imaging features of cases of surgically repaired TOF and to evaluate the relationship among data that are used in follow-up procedures such as right ventricular ejection fraction (RV-EF), PRF, and the degree of RV enlargement and dysfunction.

2. Materials and methods

2.1. Patients

This retrospective study was approved by our local ethics committee. Fourteen patients who were admitted to our clinic for CMR imaging between July 2008 and September 2011 were included in the study. The study group consisted of 9 males and 5 females, and their ages ranged between 7 and 19 years (mean age: 11.9 ± 3.6 years). All patients were surgically treated for TOF and, at the time of the operation, their ages ranged between 1 year and 4 years. Patching process was performed for RVOT and/or pulmonary annulus during full repair surgery in all patients.

2.2. CMR protocol

All examinations were performed in the supine position by using body coil and phased array coil in 1.5-T MR equipment (Siemens Symphony, Erlangen, Germany). Axial half Fourier acquisition single-shot turbo-spin echo (HASTE), true fast imaging with steady-state free precession (TrueFISP) for cine imaging, phase-contrast velocity-encoding (V_{enc}) imaging for velocity measurements, and 3-dimensional (3D) spoiled-gradient echo sequences for MR angiography were used as CMR protocol. During the imaging period, electrocardiography monitorization was performed in every patient. The 7-year-old (n = 2) and 8-year-old (n = 1) patients were scanned under general anesthesia.

At the beginning of the protocol, axial, coronal, and sagittal reference images were gained by TrueFISP sequence. This was followed by axial HASTE images that were used for revealing the general morphological features. Cine TrueFISP axial or coronal images spanning entire RV and RVOT were performed to calculate RV function in every patient. For morphological assessment, short axis, 2-, 3-, and 4-chamber planes cine TrueFISP images were obtained.

PRF measurements were performed by using the phase-contrast velocity-encoding MR imaging technique. The phase-contrast velocity-encoding imaging plane was perpendicular to the flow direction, estimated using the reference images of RVOT and the pulmonary valve in different planes. As a standard V_{enc} value, 200 cm/s was used. In the presence of aliasing artifacts, the V_{enc} value was increased by 50 cm/s. The phase-contrast velocity-encoding images were analyzed quantitatively by Argus software in a Leonardo workstation (Siemens, Erlangen, Germany). The magnitude and phase images were gained by using the flow measurement option of the software. The contour of the pulmonary valve was manually formed by using magnified magnitude images. At the point of the pulmonary valve, forward and backward flow measurements and their graphics were saved in the archive system of the hospital. PRF = backward flow (mL) / forward flow (mL) × 100 was used for calculating the PRF. PRF percentage was graded into 3 groups (grade 1: 0%–20%; grade 2: 21%–40%; grade 3: >40%).

RV functional analyses were performed by using axial images that were gained during the whole cardiac cycle in the cine TrueFISP sequence using Argus software (Leonardo, Siemens). In this assessment, end-diastolic and end-systolic contours of the right-ventricle were delineated manually in ventricle function assessment mode. End-systolic volume (ESV) and end-diastolic volume (EDV) were measured. RV-EF = (EDV – ESV/EDV) × 100 was used for calculating the RV-EF. RV-EF values higher than 45% were assumed as normal. RV dysfunction was classified into 3 groups according to RV-EF values (grade 1: 35%–45%; grade 2: 25%–34%; grade 3: <25%).

MR angiography was performed using the bolus tracking method following administration of the contrast medium by an automatic injector. The imaging was initiated after the contrast medium had reached the pulmonary artery. The sequence was repeated every 5 s after the first sequence, and at least 2 series were performed. As a consequence, besides the pulmonary artery and its branches, the aorta and its branches were also depicted. CMR sequence parameters are given in Table 1.

Table 1. Parameters of CMR sequences.

Parameters	PC MR	HASTE	TrueFISP	3D GRE T1
TR (ms)	35	800	43.26	3.44
TE (ms)	4	28	1.3	1.28
Flip angle (°)	30	160	80	30
FOV (mm)	250–360	250–360	250–360	250–360
Matrix	179 × 256	106 × 256	156 × 192	247 × 384
Slice thickness (mm)	5	5-7	5-7	1
Bandwidth (Hz/px)	279	781	965	540
NEX	3	1	1	1
Cardiac phase number	30	-	-	-
V_{enc} (cm/s)	100–350	-	-	-
Acquisition time (s)	145–190	26	14	26

TR: Repetition time, TE: Echo time, FOV: Field of view, NEX: Number of excitations, V_{enc}: Velocity encoding, PC MR: Phase-contrast magnetic resonance, HASTE: Half Fourier acquisition single-shot turbo spin echo, TrueFISP: True Fast imaging with steady-state free precession, 3D GRE: Three-dimensional gradient-recalled echo.

2.3. Statistical analysis

For discrete and continuous data, percentage and median (min-max) values were used in descriptive statistics, respectively. For comparison between groups with discrete variables and continuous variables, the chi-square and Mann–Whitney U tests were used, respectively. The changes of the degree of PRF and RV dysfunction were evaluated with Spearman's rho. All statistical analyses were done using SPSS 15.0 (SPSS for Windows; SPSS Inc., Chicago, IL, USA). P values less than 0.05 were accepted as significant.

3. Results

RV enlargement, increased trabeculation, and pulmonary regurgitation were detected in all cases (100%). There was RVOT dilatation in 10 cases (71%), flattening of the interventricular septum in 8 cases (57%), RV dysfunction in 8 cases (57%), tricuspid regurgitation in 6 cases (43%), mitral regurgitation in 2 cases (14%), left pulmonary artery stenosis in 1 case (7%), dilatation of the ascending aorta in 2 cases (14%), right aortic arch in 2 cases (14%), and myocardial crypt in 1 case (7%) (Figures 1 and 2). The imaging features of the cases are summarized in Table 2.

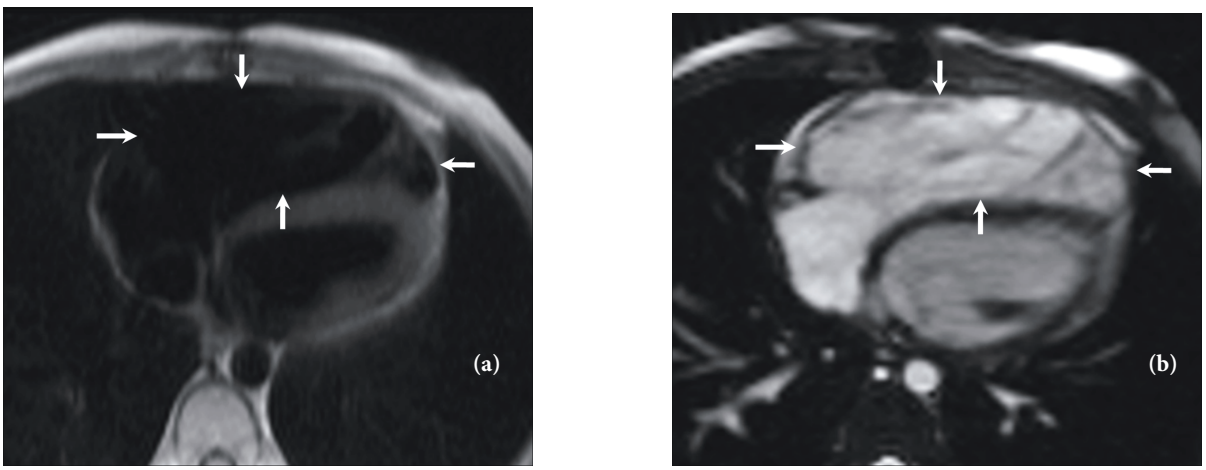

Figure 1. Axial half Fourier acquisition single-shot turbo spin echo (HASTE) **(a)** and true fast imaging with steady-state free precession (TrueFISP) **(b)** MR images obtained in an 11-year-old girl with surgically repaired TOF showing a dilated right ventricle (arrows).

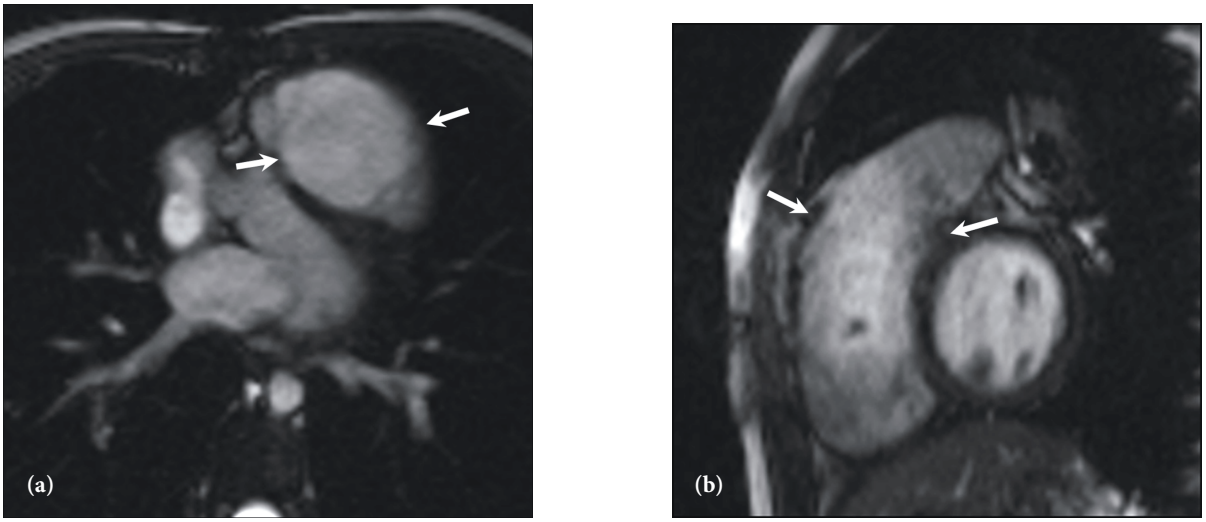

Figure 2. Axial TrueFISP image **(a)** and TrueFISP image oriented toward the RV outflow tract oblique sagittal **(b)** showing aneurysmal dilatation of the RV outflow tract (arrows) in an 11-year-old girl with surgically repaired TOF.

The PRFs ranged between 29% and 48% (mean: 41.4 ± 5.4%; median: 43%), while RV-EF values ranged between 29.3% and 58.5% (mean: 42.3 ± 9.2%; median: 43.4%) (Table 2; Figure 3).

In 9 cases (64.3%) grade 3 and in 5 cases (35.7%) grade 2 PRFs were determined. In 4 cases (28.6%) grade 1 and in 4 cases (28.6%) grade 2 RV dysfunctions were revealed according to RV-EF values. In 6 cases (42.8%) right ventricle functions were normal. There was no statistically significant relationship between degree of PRF and degree of the RV dysfunction (P = 0.147, chi-square test, Spearman's rho = –0.158).

RV dilatation was determined in all cases. RV EDV values ranged between 105.7 mL/m^2 and 211.7 mL/m^2 (mean: 153.6 ± 34 mL/m^2; median: 151.2 mL/m^2), while RV ESV values ranged between 53.3 mL/m^2 and 149.7 mL/m^2 (mean: 89.3 ± 28.2 mL/m^2; median: 83.5 mL/m^2) (Figure 4). There was no statistically significant difference between cases with and without TR according to RV EDV (P = 0.366, Mann–Whitney U test), RV ESV (P = 0.561, Mann–Whitney U test), and RV stroke volume (P = 0.439, Mann–Whitney U test) values or the grade of the right ventricular dysfunction (P = 0.823, chi-square test).

RV-EF values of 10 cases with RVOT dilatation ranged between 29.3% and 58.5%. There was no statistically significant relationship between cases with and without RVOT dilatation according to the RV-EF (P = 0.777, Mann–Whitney U test) or degree of the RV dysfunction (P = 0.052, chi-square test).

4. Discussion

The aims of TOF surgery are to repair VSD and to enlarge the RVOT (9). With recent advances in surgical techniques and postoperative follow-up, complete surgical repair has become feasible at early ages. Therefore, hypoxemia can be eliminated earlier, and normal growth and organ development has become possible (9). Postoperative complications are extremely low and most of the patients survive until adulthood. Those who survive frequently suffer from RV dilatation, dysfunction, or insufficiency and exercise intolerance due to chronic PR. The complications determined in postoperative period are residual VSD, pulmonary stenosis, PR, TR, RV dilatation-dysfunction, aneurysmatic dilatation of the RVOT, conduit obstruction, and left ventricular dysfunction.

Residual VSD is extremely rare in surgically repaired TOF cases, but it must be carefully investigated and excluded. Although residual VSDs can be accurately revealed by using 2D Doppler echocardiography, they can be also determined by using SSFP sequences. The size of the shunt can also be measured by using the phase-contrast technique. There was no residual VSD in any of the cases in our study group.

PR is the most common sequelae of the transannular patching or repair of the RVOT with patch techniques. It is encountered in almost all cases and can be accurately quantified by using phase-contrast MR technique. In addition to this, the effect of PR on RV volume and function can be measured and followed up by serial scans (9). Mild pulmonary regurgitation is frequently seen in patients with total surgical repair and is usually well tolerated (10). In cases with moderate or advanced PR, the progressive enlargement of the RV, arrhythmias during exercise, or exercise intolerance, reoperation for the repair of the PR is suggested (11).

There is no accepted guideline determining the timing of the treatment of chronic PR. CMR plays an important role in the exact quantification of the PR and RV-EF and in management of these patients. Recently, the gold standard

Table 2. CMR imaging findings of patients with TOF repair.

No./ Sex/ Age	RV enlargement	RV dysfunction	IVS flattening	RVOT dilatation	PR	Other findings	RV EDV (mL/m²)	RV ESV (mL/m²)	RV stroke volume (mL/m²)	RV-EF (%)	PRF (%)	Degree of RV dysfunction	Degree of PR fraction
1/F/7	+	+	+	+	+	-	127.4	86.2	41.2	32.3	46	2	3
2/F/13	+	+	+	+	+	TR	134.5	81.3	53.2	39.6	45	1	3
3/M/10	+	-	-	+	+	-	148.1	81.3	66.8	45.1	42	0	3
4/F/11	+	-	+	+	+	-	105.7	53.3	52.4	49.6	43	0	3
5/M/13	+	+	+	+	+	TR, aortic dilatation	211.7	149.7	62	29.3	38	2	2
6/M/16	+	+	-	-	+	-	195	125	70	35.9	36	1	2
7/M/11	+	+	+	-	+	TR	195	127	68	34.9	47	2	3
8/M/10	+	-	+	+	+	MR	133.6	55.4	78.2	58.5	45	0	3
9/M/8	+	+	-	+	+	MR, crypt	111.7	64.7	47	42.1	29	1	2
10/F/11	+	-	-	+	+	Left pulmonary artery stenosis, TR	154.3	66.9	87.4	56.6	48	0	3
11/M/16	+	-	+	-	+	TR	165	85	80	48.5	36	0	2
12/M/19	+	+	+	+	+	Right aortic arch	117	82	35	29.9	45	2	3
13/F/15	+	-	-	+	+	-	164	89	75	45.7	43	0	3
14/M/7	+	+	-	-	+	Right aortic arch, TR, aortic dilatation	187.4	103.8	83.6	44.6	37	1	2

RV: Right ventricular, IVS: Interventricular septum, EF: Ejection fraction, RVOT: Right ventricular outflow tract, PR: Pulmonary regurgitation, PRF: PR fraction, TR: Tricuspid regurgitation, MR: Mitral regurgitation, EDV: End-diastolic volume, ESV: End-systolic volume.

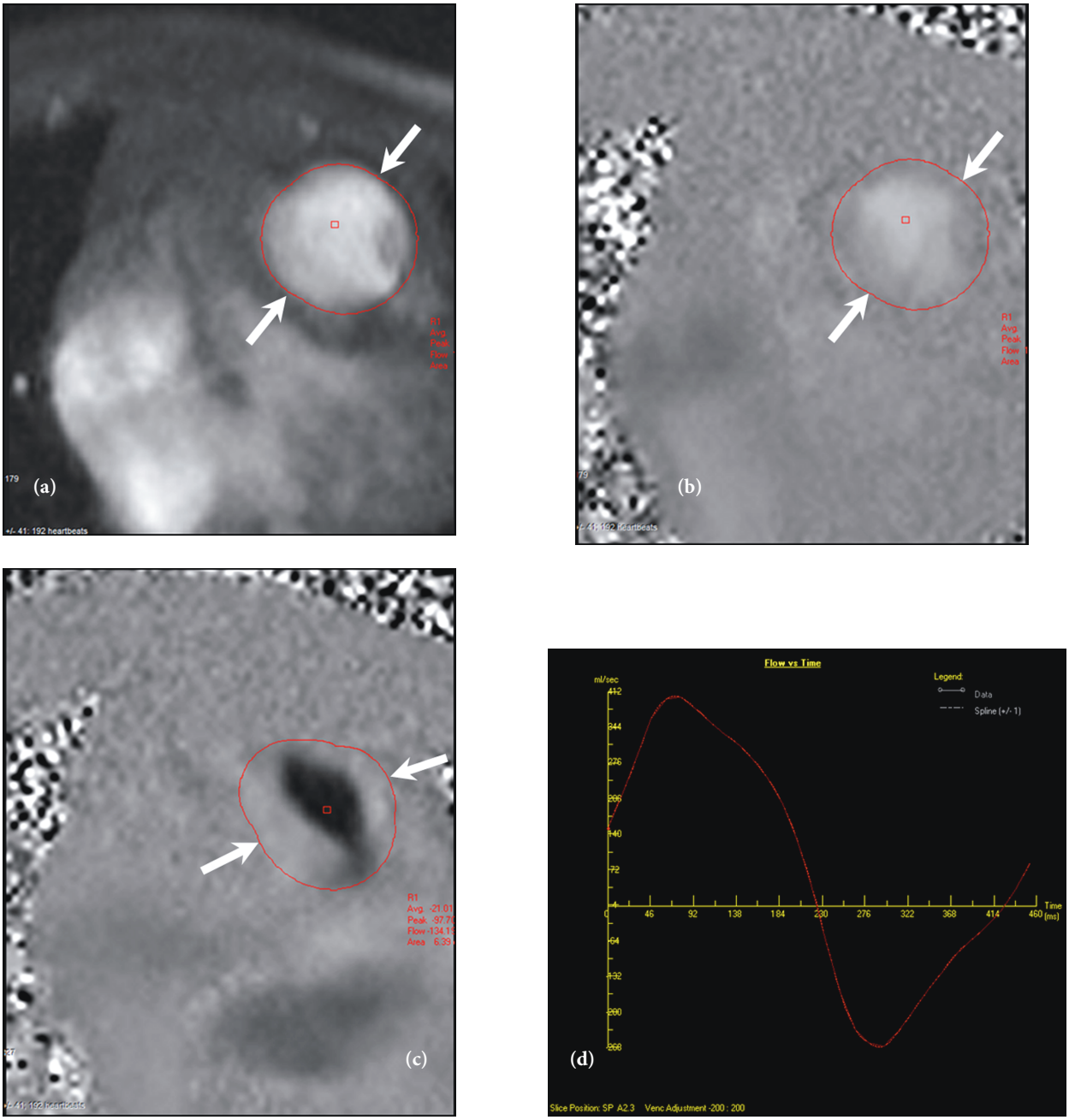

Figure 3. Magnitude image **(a)**, phase-velocity images obtained during systole **(b)** and diastole **(c)**, and graph **(d)** obtained from phase-contrast MR imaging reveal PR in a 7-year-old girl with surgically repaired TOF. Magnitude image **(a)** shows the pulmonary valve level (arrows) in cross-section. On a phase-velocity image obtained during systole **(b)**, the signal intensity of the pulmonary artery (arrows) is proportional to through-plane velocity. Phase-velocity image obtained during diastole **(c)** reveals retrograde PR flow. Graph **(d)** illustrates flow (mL/s) versus time (ms) during phase-contrast imaging. PR fraction is the ratio of retrograde flow volume (regurgitation) to antegrade flow volume. PR fraction is 46%.

in measurement of the volume and assessment of the function of the RV ventricle has become CMR. RV-EF is the most adequate and reproducible parameter with which to evaluate the RV function. Low EF is in close relationship with poor prognosis in patients with surgically repaired TOF. The early diagnosis of this condition and early interventions to protect RV function may lead to better prognosis (2,6,9). The reconservation of the pulmonary valve function decreases RV dilatation and leads to a better clinical outcome (12–15).

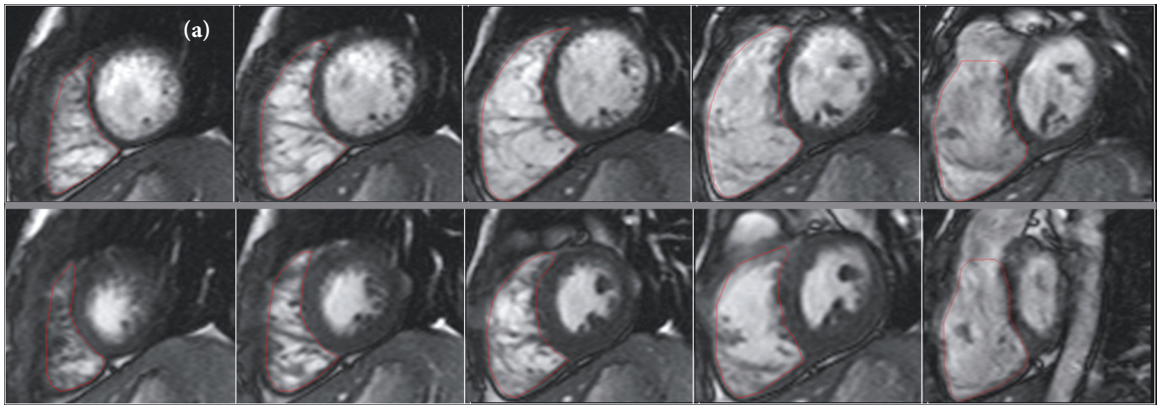

(b)

Right Ventricle - Absolute				
Cardiac Function			Normal Range (M) (MRI)	Units
Ejection Fraction	EF	35.9	47.00 ... 74.00	%
End Diastolic Volume	EDV	236.8	88.00 ... 227.00	ml
End Systolic Volume	ESV	151.8	23.00 ... 103.00	ml
Stroke Volume	SV	85.0	52.00 ... 138.00	ml
Cardiac Output	CO	----	----	l/min
Myocardial Mass (at ED)		----	----	g
Myocardial Mass (Avg)		----	----	g

(c)

Right Ventricle - Normalized				
Cardiac Function			Normal Range (M) (MRI)	Units
End Diastolic Volume	EDV	195.2	55.00 ... 105.00	ml/m^2
End Systolic Volume	ESV	125.1	15.43 ... 42.91	ml/m^2
Stroke Volume	SV	70.0	32.00 ... 64.00	ml/m^2
Cardiac Index	CI	----	----	l/min/m^2
Myocardial Mass (at ED)		----	----	g/m^2
Myocardial Mass (Avg)		----	----	g/m^2

Figure 4. Calculation of the RV EDV and ESV in a 16-year-old male with surgically repaired TOF. Multiple contiguous short-axis TrueFISP images **(a)** show the endocardial borders of the ventricular cavities in end-diastole (upper row) and in end-systole (bottom row). Graphs **(b** and **c)** show the RV EDV, ESV, stroke volume, and ejection fraction values. Absolute values and body surface area normalized values are shown in images **(b)** and (**c**), respectively.

In the follow-up of patients with surgically repaired TOF, PRF is quantified by using right ventricle volume and function. There is no classification for the degrees of the insufficiency according to PRF values. In previous studies, authors noted that an accurate classification could be achieved by using larger study groups and longer follow-up times (16–19).

Grothoff et al. (20) reported that there was no statistically significant relationship between RV-EF and PRF, but there were weak correlations among PRF, RV ESV, and EDV. Parallel to that study, we also determined that there was no correlation between degree of PRF and RV-EF value or degree of RV dysfunction. In addition, in our study group, we did not determine any correlation between PRF and the degree of the enlargement of the RV, RV ESV, or EDV. According to these results, the parameters causing morbidity in patients with surgically repaired TOF such as PR, RV enlargement, decrease in RV-EF, and RV dysfunction have a cause-and-effect relationship, but there is no reliable and statistically significant correlation among them. As an example, the effect of PR on RV enlargement also depends on the duration of the chronic PR, RV myocardial mass, and contractibility, in addition to the degree of the PR. Therefore, in addition to clinical data, the follow-up of these parameters in each case by serial scans has an important role in the management of these patients.

The leading causes of PR in TOF patients are disruption of pulmonary valve integrity and enlargement of the RVOT after the surgical correction operation. The operation technique is also important. For example, with the transannular patching technique, the probability of PR is higher than in other techniques (20). PR causes dysfunction of the RV due to volume overload. One of the causes of RV volume overload is tricuspid insufficiency, which was seen in 43% of our cases. On the other hand, RV volume overload is reported to be well tolerated for a long duration (a few decades) without causing RV dysfunction (21). In our study, there was no correlation between PRF and RV dysfunction, and we considered that this may be due to operation technique, coexisting pathologies that may lead to RV volume overload (such as tricuspid insufficiency or atrial septal defect), or duration of the chronic PR.

The prevalence of moderate or advanced TR is estimated at 10% in patients with surgically repaired TOF. It is reported that TR is usually a result of progressive RV dilatation followed by annular dilatation of the tricuspid valve. In our study group, we determined TR in 6 cases (43%). There was RV enlargement in every patient, but in contrast to previous literature, the enlargement was not more prominent in cases with TR when compared to cases without TR.

RVOT enlargement usually occurs in patients with surgically repaired TOF and is related to transannular or RVOT patching techniques. Other factors related to this complication are large amount of infundibular muscle resection and ischemia (22). The size of the RVOT aneurysm can be readily and precisely evaluated by cine SSFP images. Presence of the RVOT aneurysm was reported to be in relation with decreased RV-EF (22). However, in our study, there was no significant difference between RV-EF values of cases with or without RVOT dilatation.

The major limitations of this study are its retrospective design and relatively low number of cases. Another limitation is the lack of echocardiographic and clinic data in some patients and lack of comparison of these data with CMR findings. In prospective studies with serial CMR scans proven by the clinical and echocardiographic findings, the relationship of the PRF with RV size, EF, degree of dysfunction, and clinical findings can be more accurately evaluated, and the parameters and quantitative values for optimal timing for pulmonary valve replacement can be determined.

In conclusion, besides the morphological assessment of cases with surgically repaired TOF, CMR also allows for measuring quantitative parameters such as PRF and RV-EF (RV function/dysfunction) and depicting the possible complications of the procedure. Although PR is the leading cause of RV dilatation and dysfunction in these patients, the degree of PR is not always correlated with the degree of RV dysfunction.

References

1. Kula S, Çevik A, Olguntürk FR, Tunaoğlu FS, Oğuz AD, İlhan MN. Distribution of congenital heart disease in Turkey. Turk J Med Sci 2011; 41: 889–93.
2. Helbing WA, de Roos A. Clinical applications of cardiac magnetic resonance imaging after repair of tetralogy of Fallot. Pediatr Cardiol 2000; 21: 70–9.
3. Blalock A, Taussig HB. The surgical treatment of malformation of the heart in which there is pulmonary stenosis or pulmonary atresia. JAMA 1945; 128: 189–202.
4. Lillehei CW, Cohen M, Warden HE, Read RC, Aust JB, Dewall RA et al. Direct vision intracardiac surgical correction of the tetralogy of Fallot, pentalogy of Fallot, and pulmonary atresia defects; report of first ten cases. Ann Surg 1955; 142: 418–42.
5. Nollert G, Fischlein T, Bouterwek S, Bohmer C, Klinner W, Reichart B. Long-term survival in patients with repair of tetralogy of Fallot: 36-year follow-up of 490 survivors of the first year after surgical repair. J Am Coll Cardiol 1997; 30: 1374–83.
6. Geva T. Repaired tetralogy of Fallot: the roles of cardiovascular magnetic resonance in evaluating pathophysiology and for pulmonary valve replacement decision support. J Cardiovasc Magn Reson 2011; 13: 9.
7. Duarte R, Fernandez-Perez G, Bettencourt N, Sampaio F, Miranda D, França M et al. Assessment of left ventricular diastolic function with cardiovascular MRI: what radiologists should know. Diagn Interv Radiol 2012; 18: 446–53.
8. Hazirolan T, Taşbaş B, Dağoğlu MG, Canyiğit M, Abali G, Aytemir K et al. Comparison of short and long axis methods in cardiac MR imaging and echocardiography for left ventricular function. Diagn Interv Radiol 2007; 13: 33–8.
9. Norton KI, Tong C, Glass RB, Nielsen JC. Cardiac MR imaging assessment following tetralogy of Fallot repair. Radiographics 2006; 26: 197–211.
10. Poirier RA, McGoon DC, Danielson GK, Wallace RB, Ritter DG, Moodie DS et al. Late results after repair of tetralogy of Fallot. J Thorac Cardiovasc Surg 1977; 73: 900–8.
11. Horneffer PJ, Zahka KG, Rowe SA, Manolio TA, Gott VL, Reitz BA et al. Long-term results of total repair of tetralogy of Fallot in childhood. Ann Thorac Surg 1990; 50: 179–83.
12. Discigil B, Dearani JA, Puga FJ, Schaff HV, Hagler DJ, Warnes CA et al. Late pulmonary valve replacement after repair of tetralogy of Fallot. J Thorac Cardiovasc Surg 2001; 121: 344–51.
13. Therrien J, Provost Y, Merchant N, Williams W, Colman J, Webb G. Optimal timing for pulmonary valve replacement in adults after tetralogy of Fallot repair. Am J Cardiol 2005; 95: 779–82.
14. Buechel ER, Dave HH, Kellenberger CJ, Dodge-Khatami A, Pretre R, Berger F et al. Remodelling of the right ventricle after early pulmonary valve replacement in children with repaired tetralogy of Fallot: assessment by cardiovascular magnetic resonance. Eur Heart J 2005; 26: 2721–7.
15. Geva T, Gauvreau K, Powell AJ, Cecchin F, Rhodes J, Geva J et al. Randomized trial of pulmonary valve replacement with and without right ventricular remodeling surgery. Circulation 2010; 122: 201–8.
16. Cheung EW, Wong WH, Cheung YF. Meta-analysis of pulmonary valve replacement after operative repair of tetralogy of Fallot. Am J Cardiol 2010; 106: 552–7.
17. Warner KG, O'Brien PK, Rhodes J, Kaur A, Robinson DA, Payne DD. Expanding the indications for pulmonary valve replacement after repair of tetralogy of Fallot. Ann Thorac Surg 2003; 76: 1066–71.

18. Lurz P, Giardini A, Taylor AM, Nordmeyer J, Muthurangu V, Odendaal D et al. Effect of altering pathologic right ventricular loading conditions by percutaneous pulmonary valve implantation on exercise capacity. Am J Cardiol 2010; 105: 721–6.

19. Tsang FH, Li X, Cheung YF, Chau KT, Cheng LC. Pulmonary valve replacement after surgical repair of tetralogy of Fallot. Hong Kong Med J 2010; 16: 26–30.

20. Grothoff M, Spors B, Abdul-Khaliq H, Gutberlet M. Evaluation of postoperative pulmonary regurgitation after surgical repair of Fallot: comparison between Doppler echocardiography and MR velocity mapping. Pediatr Radiol 2008; 38: 186–91.

21. Shimazaki Y, Blackstone EH, Kirklin JW. The natural history of isolated congenital pulmonary valve incompetence: surgical implications. Thorac Cardiovasc Surg 1984; 32: 257–9.

22. Davlouros PA, Kilner PJ, Hornung TS, Li W, Francis JM, Moon JC et al. Right ventricular function in adults with repaired tetralogy of Fallot assessed with cardiovascular magnetic resonance imaging: detrimental role of right ventricular outflow aneurysms or akinesia and adverse right-to-left ventricular interaction. J Am Coll Cardiol 2002; 40: 2044–52.